COMPUTATIONAL TECHNIQUE FOR PREDICTING PROPERTIES OF POLYMER MATRIX COMPOSITES

Author, co-author (Do NOT enter this information. It will be pulled from participant tab in MyTechZone)

Affiliation (Do NOT enter this information. It will be pulled from participant tab in MyTechZone)

Abstract

Hybrid natural fibre polymer composites have attracted significant attention from the research community owing to their better mechanical properties and eco-friendly nature as compared to conventional materials. Abaca, in particular, has shown tremendous potential for its suitability in structural applications. This present work deals with the mechanical characterization and modelling of hybrid abaca-epoxy composites with red mud as a filler. Hybrid composites were prepared by the hand lay-up technique; preliminary experiments involving banana and sisal were also performed to understand the composite fabrication procedure. Experiments for the primary study were designed based on a full factorial method having three control parameters: weight percentage of abaca (2.6, 5.26, and 7.9 wt%), weight percentage of red mud (4, 8, and 12 wt%), and particle size of red mud (68, 82, and 98 mm). The flexural and impact strengths of the composites were evaluated. To further analyze the dataset, find the optimized parameter values, and gather different data insights regarding the input and output parameters, three optimization algorithms—Genetic Algorithm (GA), Grey Wolf Optimizer (GWO), and Differential Evolution (DE)—were employed. This study provides a comprehensive analysis of the composite's mechanical behavior and identifies the optimal formulation for improved performance through a comparative algorithmic approach.

Keywords: Hybrid Composites, Natural Fibre Composites, Abaca, Epoxy, Red Mud, Mechanical Properties, Flexural Strength, Impact Strength, Full Factorial Design, Optimization, Genetic Algorithm (GA), Grey Wolf Optimizer (GWO), Differential Evolution (DE), Hand Lay-up**Introduction.**

Introduction

The transition toward sustainable and eco-friendly materials has intensified interest in natural fiber composites (NFCs) as alternatives to conventional synthetic composites. Plant-based fibers such as flax, jute, hemp, sisal, coir, kenaf, and abaca are widely used in NFCs because of their renewability, low cost, biodegradability, and favorable specific strength [1], [2]. These composites are lightweight and environmentally benign, making them attractive for applications in automotive, construction, packaging, and consumer products [3].Despite these advantages, NFCs face persistent challenges such as poor fiber–matrix adhesion, moisture sensitivity, and variability in performance [4], [5]. while hybridization of natural fibers with each other or with synthetic fibers has shown improved strength and durability [2], [5]. More recently, nanotechnology approaches, including the incorporation of graphene and nanocrystalline cellulose, have further enhanced the stiffness, toughness, and thermal stability of NFCs [6], [7]. NFCs reinforced with fibers such as flax, hemp, jute, sisal, kenaf, and abaca are no longer limited to specialized applications but are emerging as mainstream solutions for sustainable engineering [8].

Abaca (*Musa textilis*) fibers, recognized for their high tensile strength and resistance to seawater degradation, have received considerable attention as reinforcements in polymer composites. Studies confirm their effectiveness in both thermoset and thermoplastic matrices, where they improve stiffness, tensile, and flexural strength while maintaining low density and biodegradability [9–11]. Alkaline treatment has been widely adopted to enhance fiber–matrix interfacial bonding by removing hemicellulose and lignin, which improves crystallinity and reduces moisture uptake [10,17]. Hybridization of abaca with glass, jute, and raffia fibers has also shown notable improvements in toughness, impact resistance, and dimensional stability [12-13]. Furthermore, investigations into viscoelastic properties demonstrate that hybrid abaca composites exhibit enhanced storage modulus and damping behavior, highlighting their potential in dynamic applications [14]. In thermoplastic matrices such as bio-polyethylene (BioPE), abaca fiber reinforcement has been reported to significantly enhance flexural and tensile properties, positioning it as a competitive candidate for sustainable plastics [15,16]. Recent approaches have also emphasized eco-friendly processing, including alkali treatment systems with chemical recirculation to reduce environmental impact while maintaining material performance [17]. Collectively, abaca fiber composites have advanced from exploratory studies to practical applications, with ongoing research emphasizing hybridization, surface treatment, and sustainable processing for improved performance and circularity.

Red mud—an iron-oxide–rich byproduct of alumina refinement—presents a sustainable and cost-effective filler for composites, particularly useful when integrated into polymer matrices with natural fibers. Rajendran et al. demonstrated that polyester composites reinforced with jute fibers and red mud (10–30 wt. %) showed enhanced erosion resistance and surface hardness, especially when fibers underwent NaOH or silane treatment to improve adhesion [18]. Melnyk’s study using glyptal resin composites with up to 56 wt.% red mud found that in-situ incorporation at around 36 wt.% boosted impact strength by 12.5% compared to mechanical mixing (impact strength reached 22.05 N·m) [19]. Dos Santos and colleagues investigated hybrid polyester composites combining bamboo fibers and 30 wt.% red mud—they observed a flexural strength of 124.7 MPa (an increase of ~149%) and a 68% increase in tensile strength compared to matrices without red mud [20].

Collectively, these findings underscore red mud's ability to enhance mechanical and erosion-related properties in eco-friendly composites, particularly when fillers are properly treated or introduced in situ at moderate loadings (around 30–40 wt. %) for optimal performance and processability.

The design and optimization of composite materials often involve multiple interacting factors such as reinforcement type, filler content, processing conditions, and temperature, which exhibit nonlinear and synergistic effects on performance outcomes like strength, stiffness, and durability. Response Surface Methodology (RSM) has emerged as a powerful statistical and mathematical framework to efficiently model such complex relationships, enabling the generation of second-order polynomial models with relatively few experimental runs and providing clear visualization of input–output interactions through contour and surface plots [21]. Originally developed by Box and Wilson in the 1950s, RSM has since become a cornerstone in engineering optimization using designs like Central Composite Design (CCD) and Box–Behnken Design (BBD) that strike a balance between precision and resource requirements [22]. In the field of composites, RSM has been successfully applied to optimize fiber-reinforced polymer composites [23], hybrid laminates combining natural and synthetic fibers [24], and eco-friendly plant fiber composites [25]. Studies have also demonstrated the effectiveness of RSM in modeling ceramic-filled polyester resin composites [26], nanofiller-augmented composites [27], Overall, RSM provides not only cost-effective experimental optimization but also deep insight into the factor–response landscape of composite materials, guiding efficient material development and performance improvement [28].

Optimization of composite materials has been widely studied using a variety of algorithms and hybrid strategies. Sebaey et al. applied an Ant Colony Optimization (ACO) framework to dispersed laminated composite panels under biaxial loading to identify ply-angle configurations that maximize buckling resistance and improve the strength/weight trade-off. They encoded continuous fiber orientations as the search space and validated the ACO-derived layups with finite-element checks, reporting significant buckling improvements over conventional symmetric layups [29]. Hwang et al. implemented a Genetic Algorithm (GA) tailored for fiber-angle optimization in laminated composites, incorporating adaptive crossover and mutation strategies to enhance hill-climbing while preserving diversity. Their GA-based designs produced layups with higher bending stiffness and buckling load compared with deterministic or fixed-angle designs, demonstrating the benefit of adaptive genetic operators for discrete ply-angle problems [30]. Le-Manh et al. developed a GA + isogeometric analysis (IGA) pipeline for stacking-sequence optimization targeted at maximizing strength and stiffness of laminated composite plates. The coupling of GA search with NURBS-based IGA allowed accurate gradient-free exploration of ply sequences, and the optimized laminates exhibited improved strength and modal characteristics versus baseline configurations [31]. Ho-Huu and Nguyen proposed an improved Differential Evolution (DE) hybridized with a smoothed finite-element method to maximize buckling loads of laminated plates. The hybrid DE approach sped up convergence and found higher-critical-load stacking sequences than classical DE and some GA baselines, validating the value of DE variants in continuous laminate optimization tasks [32]. Cakiroglu et al. applied Harmony Search (a music-inspired metaheuristic) to optimize ply angles of dispersed laminated composites for buckling performance. The harmony-search-optimized laminates achieved buckling loads comparable to GA-optimized designs, showing that diverse bio-inspired optimizers can be competitive alternatives for ply-angle tuning under geometric/manufacturing constraints [33]. Arjomandi et al. used Particle Swarm Optimization (PSO) to optimize the layup of carbon/epoxy double-lap composite joints with the explicit goal of minimizing peak interlaminar stresses and enhancing joint strength. By encoding ply orientation and stacking order in PSO particles and coupling with FEA, the authors reported reduced stress concentrations and improved failure loads compared with conventional layups [34]. Wang and Wu presented a decade-review of Genetic Algorithm applications in composite materials and structures, cataloguing GA encodings, fitness definitions (stiffness, strength, buckling), and common hybridizations (local search, surrogate models). Their synthesis concluded that GAs remain especially effective for discrete stacking-sequence problems and when manufacturing constraints must be embedded directly in the search [35]. Emambocus et al. surveyed the Dragonfly Algorithm (DA) and its hybrid variants, discussing DA's exploration–exploitation mechanisms and recommended DA hybridizations for structural and composite design problems. They identified DA's discrete-search adaptations (e.g., angle modulation) as particularly useful for ply-sequence and on/off composite-placement decisions [36]. Parmaksiz et al. proposed a Mutation-based Improved Dragonfly Algorithm (MIDA) and tested it on engineering benchmarks to demonstrate improved convergence, stability, and accuracy. They suggested MIDA as a promising candidate for high-dimensional, multi-modal composite design optimization (for example, fiber-volume fraction and multi-objective strength/stiffness trade-offs) [37]. Wang, Shi and Zhang introduced an angle-modulated Dragonfly Algorithm (AMDA) that converts continuous DA outputs into binary or discrete decisions via angle modulation. They demonstrated AMDA on combinatorial engineering problems and recommended it for discrete laminate stacking and binary fiber-placement tasks where DA's continuous form is insufficient [38]. Liu et al. presented a parallel evolutionary layup-optimization method aimed at matching target lamination parameters (macroscopic stiffness targets). The parallelization and tailored fitness allowed the method to produce laminate stacking sequences that matched desired stiffness tensors with fewer high-fidelity evaluations, enabling faster design for tailored stiffness composites [39]. Zadeh and colleagues developed a bi-level optimization scheme for symmetric composite structures in which the upper level minimized weight while the lower level enforced manufacturable ply-sequence and strength constraints. The bi-level approach produced lightweight yet manufacturable laminates that met structural targets and reduced the complexity of direct multi-objective search [40]. Keshtegar et al. combined adaptive Kriging surrogate models with an improved particle-swarm optimizer to maximize buckling loads of laminates, demonstrating that surrogate-assisted PSO significantly reduced expensive FEA calls while maintaining the quality of the Pareto front for multi-objective laminate design [41]. Malashin et al. used evolutionary multi-objective search to tune neural-network surrogates that predict textile-composite properties; joint optimization of NN hyperparameters and training data selection improved surrogate fidelity and yielded better optimization outcomes for modulus and strength objectives in textile composites [42]. Yibre and Tekalign applied an Artificial-Algae Algorithm to weight-optimize hybrid laminates, demonstrating that newer bio-inspired optimizers can match or exceed GA/PSO performance in producing lightweight stacks that preserve required stiffness metrics, particularly when objective landscapes are highly multimodal [43]. Işık et al. developed a hybrid ANN–PSO framework in which an ANN surrogate predicts composite mechanical responses and PSO performs the search for optimal layups. The authors reported large reductions in full FEA

runs while finding designs with improved stiffness and natural-frequency characteristics compared to unoptimized laminates [44].Qu, Liu and Cao presented an Adaptive Surrogate-Assisted PSO (ASAPSO) combining global and local surrogate models and applied it to medium-scale engineering optimization tasks. They demonstrated ASAPSO's ability to conserve high-fidelity evaluations while achieving strong optimization outcomes — a pattern directly applicable to expensive composite FEA-based searches [45]. Yue et al. used PSO within an ultrasonic guided-wave damage-imaging framework to locate damage in composite plates; while not purely a layup-optimization study, their work shows PSO's practical utility in inverse problems for composites, where mechanical response data (guided waves) drive parameter identification for defects that affect mechanical properties [46]. Li et al. proposed a Fast Surrogate-Assisted Particle Swarm Optimization (FSAPSO) for computationally expensive engineering design and validated it on benchmark problems; the FSAPSO framework — when transferred to composite material design — enables rapid optimization of parameters like fiber volume fraction, dispersion, and ply orientation while minimizing expensive FEA/experiments [47].

OBJECTIVE

This research addresses a twofold problem: a methodological limitation in traditional modeling and a material knowledge gap. Standard statistical methods like ANOVA and RSM are often limited to finding local optimums, as their polynomial models fail to capture the complex, non-linear interactions within advanced composites. This is coupled with a specific lack of scientific data on the synergistic effects of combining abaca fibre and red mud filler. It is currently unknown how these two materials interact to influence the final mechanical properties, a gap this study aims to fill by using advanced computational optimization techniques better suited for identifying the true global optimum.

1. To employ advanced heuristic algorithms—namely Genetic Algorithm (GA), Grey Wolf Optimizer (GWO), and Differential Evolution (DE)—to optimize the mechanical properties (flexural strength and impact strength) of the abaca–red mud–epoxy composite.

2. To utilize these computational techniques to navigate the complex, non-linear interactions within the experimental dataset, overcoming the limitations of traditional models (like RSM/ANOVA) to find the true global optimum formulation.

3. To conduct a comparative analysis of the solutions derived from GA, GWO, and DE to evaluate their respective performance and efficiency in solving this materials optimization problem.

4. To validate the computational findings and demonstrate the superior optimization capabilities of these heuristic methods compared to traditional statistical approaches.

Methodology

An hybrid ABACA reinforced polymer composite using RSM was constructed to determine the flexural and impact strength. The below table was refered from Sinha et al.

The optimization problem aims to predict and maximize the mechanical performance of hybrid abaca–red mud–epoxy composites by identifying optimal combinations of:

- Abaca fibre weight percentage, $\boldsymbol{A}$
- Red mud filler weight percentage, $\boldsymbol{B}$
- Red mud particle size, $\boldsymbol{C}$

The objective functions correspond to:

- Flexural strength, $\boldsymbol{F(A,B,C)}$
- Impact strength, $\boldsymbol{I(A,B,C)}$

These functions were evaluated using experimentally obtained data and modeled through heuristic optimization algorithms. The design variables were constrained within experimentally validated bounds:

$$\mathbf{2.6} \leq \boldsymbol{A} \leq \mathbf{7.9}\ (wt.\%\ Abaca)\ \mathbf{4} \leq \boldsymbol{B} \leq \mathbf{12}\ (wt.\%\ Red\ Mud)\ \mathbf{68} \leq \boldsymbol{C} \leq \mathbf{98}\ (\boldsymbol{\mu m})$$

The optimization objective was formulated as a maximization problem:

$$\boldsymbol{max}\ \{\boldsymbol{F(A,B,C)},\ \boldsymbol{I(A,B,C)}\}$$

S. no	A (Wt. % of ABACA fibre)	B (Wt.% of Redmud)	C (Particle size of Redmud)	F (Flexural strength) MPa	I (Impact strength) Joule/meter
1	2.6	4	68	41.55	30.83
2	2.6	4	82	40.56	30.1
3	2.6	4	98	38.29	28.56

4	2.6	8	68	47.9	32.91
5	2.6	8	82	46.62	32.31
6	2.6	8	98	44.29	32.08
7	2.6	12	68	50.29	34.18
8	2.6	12	82	48.89	33.95
9	2.6	12	98	48.34	33.72
10	5.26	4	68	36.54	33.7
11	5.26	4	82	35.46	32.9
12	5.26	4	98	32.28	30.4
13	5.26	8	68	36.25	40.95
14	5.26	8	82	34.35	39.89
15	5.26	8	98	35.94	36.19
16	5.26	12	68	36.89	42.68
17	5.26	12	82	35.51	41.07
18	5.26	12	98	35.43	40.9
19	7.9	4	68	40.25	41.96
20	7.9	4	82	38.73	41.08
21	7.9	4	98	38.09	39.59
22	7.9	8	68	43.78	42.62
23	7.9	8	82	41.31	40.54
24	7.9	8	98	41.22	39.05
25	7.9	12	68	45.86	41.5
26	7.9	12	82	43.46	41.5
27	7.9	12	98	40.6	37.92

Genetic Algorithm (GA)

Genetic Algorithm is an optimization technique inspired by Darwin's theory of natural evolution . It works by evolving a population of solutions through a process of selection, crossover, and mutation. Over successive generations, the population "evolves" toward the best (optimal) solution .

Functions of GA:

- Selection – Chooses the fittest individuals from the population for reproduction.
- Crossover (Recombination) – Combines two parent solutions to form new offspring.
- Mutation – Introduces small random changes to maintain diversity and avoid local minima.
- Fitness Evaluation – Measures how good a solution is with respect to the objective function.

Replacement – Forms the next generation by replacing weaker solutions with stronger ones.

The Genetic Algorithm (GA) flow chart in Figure 4.2.1 outlines the steps for optimizing a solution using evolutionary principles. The process starts by randomly initializing a population within defined bounds and evaluating fitness based on *flexural* and *impact strength*. The population is sorted by fitness, and the best solution is preserved through elitism. New individuals are generated using selection (tournament method), crossover (probability 0.8), and mutation (probability 0.1). Offspring are adjusted to stay within bounds and added to form the new population, which replaces the old one in each generation. After several generations, the algorithm returns the best solution (A, B, C) and their predicted strengths.

Genetic Operators

Genetic Algorithm is an optimization technique inspired by Darwin's theory of natural evolution. It works by evolving a population of solutions through a process of selection, crossover, and mutation. Over successive generations, the population "evolves" toward the best (optimal) solution

Selection:

Tournament selection was employed, where individuals with higher fitness have a greater probability of selection.

Crossover:
Single-point crossover was applied with crossover probability $\boldsymbol{P_c = 0.8}$, producing offspring as:

$$\boldsymbol{x}_{child1} = \boldsymbol{\alpha x}_{parent1} + (\boldsymbol{1-\alpha})\boldsymbol{x}_{parent2}\ \boldsymbol{x}_{child2} = (\boldsymbol{1-\alpha})\boldsymbol{x}_{parent1} + \boldsymbol{\alpha x}_{parent2}$$

where $\boldsymbol{\alpha} \in [\mathbf{0}, \mathbf{1}]$.

Mutation:
Mutation introduces random perturbations to maintain population diversity:

$$\boldsymbol{x_{ij}^{mut}} = \boldsymbol{x_{ij}} + \boldsymbol{\delta}$$

where $\delta$is a small random number, applied with mutation probability $\boldsymbol{P_m} = \mathbf{0.1}$.

Parameter	Value
Population size	**50**
Number of generations	**100**
Crossover probability	**0.8**
Mutation probability	**0.1**
Selection method	**Tournament**
Elitism	**Enabled**

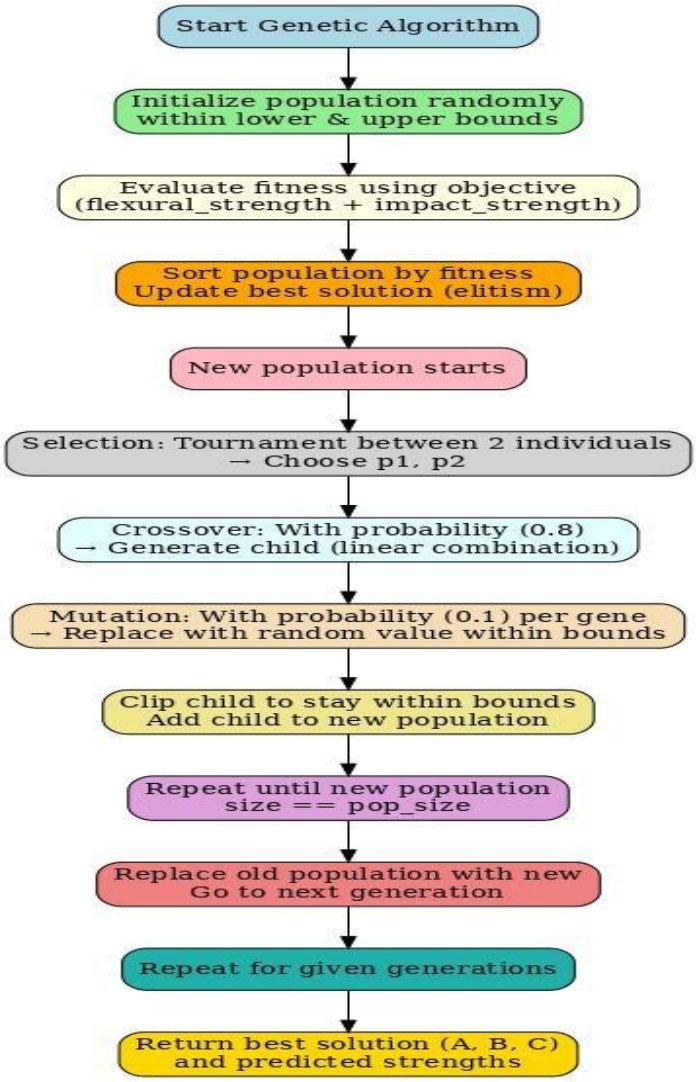

Figure 4.1 Pseudo Code using GA for optimization

Differential Evolution Algorithm (DE):

Differential Evolution is a population-based optimization algorithm used for solving complex continuous optimization problems. It operates by iteratively improving a population of candidate solutions through mutation, crossover, and selection. DE is known for its simplicity, efficiency, and strong global search capability.

Functions of DE:

- Initialization – Generates an initial population of random candidate solutions within defined bounds.
- Mutation – Creates a mutant vector by adding the weighted difference between two population vectors to a third vector.
- Crossover (Recombination) – Combines the mutant vector with a target vector to produce a trial vector, introducing variation.

- Selection – Compares the trial vector with the target vector and retains the one with better fitness for the next generation.

- Iteration (Evolution) – Repeats the process until a stopping criterion (e.g., maximum generations or convergence) is met, leading to the optimal solution.

The Differential Evolution (DE) flow chart shown in Figure 4.3.1 depicts the optimization process based on population evolution. It begins by randomly initializing a population within the given bounds, followed by evaluating the fitness of everyone using an objective function. The population is then sorted by fitness, and the best solution is stored. A new generation is created through mutation, crossover, and selection. During mutation, three distinct vectors are chosen to generate a mutant vector using a weighted difference. In the crossover step, elements from the mutant and target vectors are combined based on a crossover rate (CR). Finally, selection replaces the target vector with the mutant if it shows improved fitness. This process is repeated for all individuals until the optimal solution is obtained.

Algorithmic Framework

Differential Evolution (DE) optimizes candidate solutions through vector differentials. Each target vector is defined as:

$\mathbf{x}ig=[Aig,Big,Cig]$

where $g$denotes the generation number.

Mutation Operation

A mutant vector is generated as:

$\mathbf{v}ig=\mathbf{x}r1g+F\cdot(\mathbf{x}r2g-\mathbf{x}r3g)$

where:

- $r1,r2,r3$are distinct random indices
- $F$is the mutation scaling factor

Crossover Operation

Trial vectors are formed using binomial crossover:

$uijg=ijg$,if $randj\leq CRxijg$,otherwise

where:

- $CR$is the crossover rate
- $rand_j \in [0,1]$

Selection Criterion

$$x_i^{g+1} = \{u_i^g, if\ f(u_i^g) \geq f(x_i^g)\ x_i^g, otherwise$$

Parameter	Value
Population size	50
Scaling factor (F)	0.5
Crossover rate (CR)	0.7
Generations	100

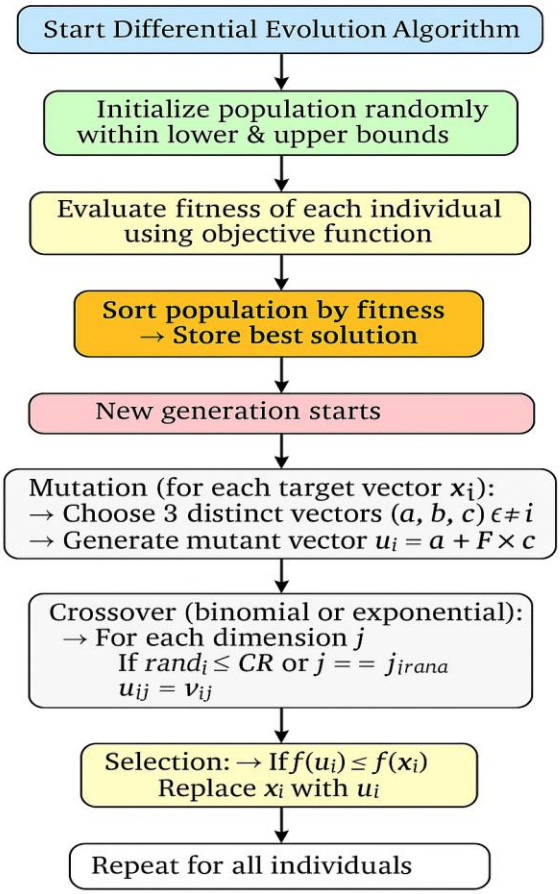

Figure 4.2 Pseudo Code using DE for optimization

Gray Wolf Optimization (GWO)

Gray Wolf Optimization is a nature-inspired metaheuristic algorithm that mimics the social hierarchy and hunting behavior of gray wolves in the wild. It is primarily used for solving complex optimization problems by balancing exploration and exploitation effectively.

Functions of GWO:

- Initialization – Generates an initial population of gray wolves (candidate solutions) randomly within the search space.
- Hierarchy Formation – Assigns leadership roles: alpha (best solution), beta (second best), delta (third best), and omega (remaining wolves).
- Encircling Prey – Wolves update their positions by surrounding the prey (optimal solution) based on alpha, beta, and delta guidance.
- Hunting – Wolves follow the top three leaders to search for prey, guiding the population toward promising regions of the search space.
- Attacking (Convergence) – As iterations progress, the wolves close in on the prey, refining the solutions and converging to the global optimum.

The Grey Wolf Optimization (GWO) flow chart shown in Figure 4.4.1 illustrates the step-by-step process of simulating grey wolf leadership and hunting behavior for optimization. The algorithm begins by randomly initializing a population within defined bounds, followed by evaluating the fitness of everyone using an objective function. The population is then sorted by fitness, and the best solutions representing the alpha (α), beta (β), and delta (δ) wolves are stored. A new generation starts where the positions and fitness of these three leading wolves are used to guide the mutation and position update of the rest of the population. Everyone's position is updated based on the influence of α, β, and δ, simulating the hunting mechanism of wolves encircling prey. The new fitness values are then evaluated, and the process continues until the termination condition is met, resulting in the optimal solution.

Algorithmic Framework

Grey Wolf Optimization (GWO) simulates the leadership hierarchy and hunting behavior of grey wolves. The population is divided into:

- α: best solution
- β: second best
- δ: third best
- ω: remaining solutions

Encircling Mechanism

The position update equations are:

$$D_\alpha = | C_1 \cdot X_\alpha - X | \quad D_\beta = | C_2 \cdot X_\beta - X | \quad D_\delta = | C_3 \cdot X_\delta - X | \quad X_1 = X_\alpha - A_1 \cdot D_\alpha \quad X_2 = X_\beta - A_2 \cdot D_\beta \quad X_3 = X_\delta - A_3 \cdot D_\delta \quad X(t+1) = \frac{X_1 + X_2 + X_3}{3}$$

where:

$$A = 2a \cdot r_1 - a, C = 2r_2$$

and $a$decreases linearly from 2 to 0 over iterations.

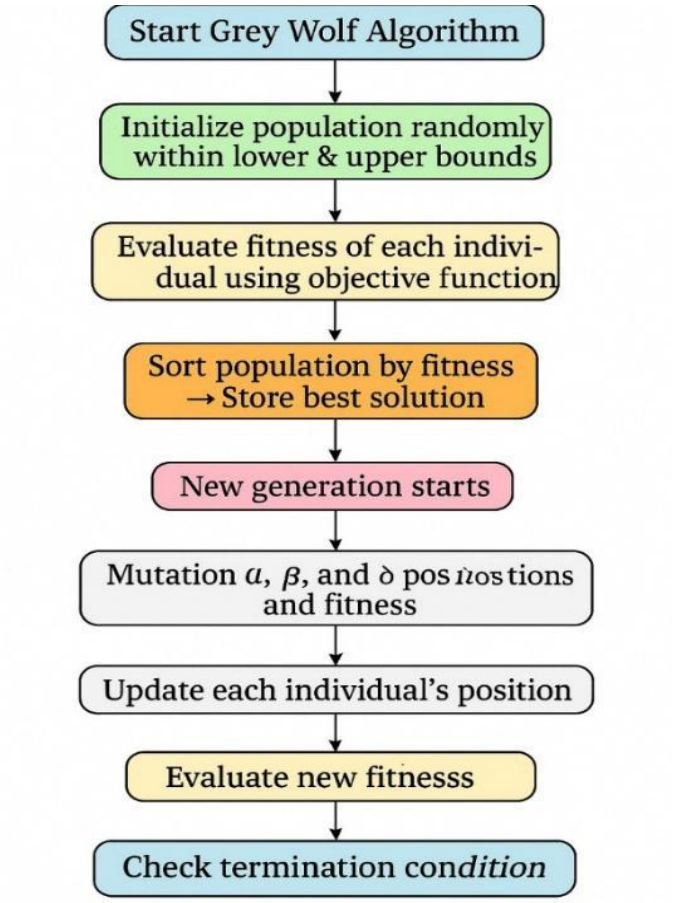

Figure 4.3 Pseudo Code using GWO for optimization

Results, Discussion and Algorithmic interpretation

Distribution and Quality of Experimental Data

Figures 5.1 (a) and (b) show the input histograms for the weight percentages of *Abaca fibre* and *Red Mud* used in the experimental dataset, while Figure 5.1 (c) represents the distribution of *Red Mud particle size*.These plots confirm that the data were uniformly distributed across the three levels of each factor: Abaca (2.6 %, 5.26 %, 7.9 %), Red Mud (4 %, 8 %, 12 %), and particle size (68 µm, 82 µm, 98 µm).

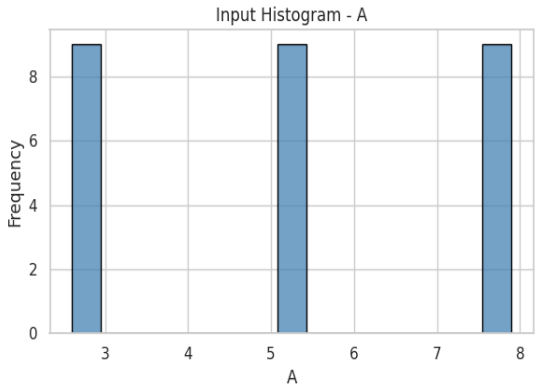

Figure 5.1. (a) Input histogram of Wt.% of abaca

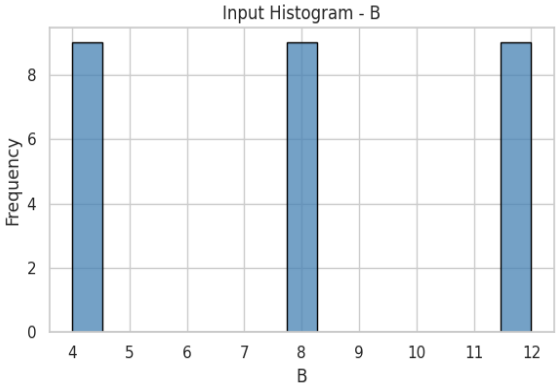

Figure 5.1. (b) Input histogram of Wt.% red mud

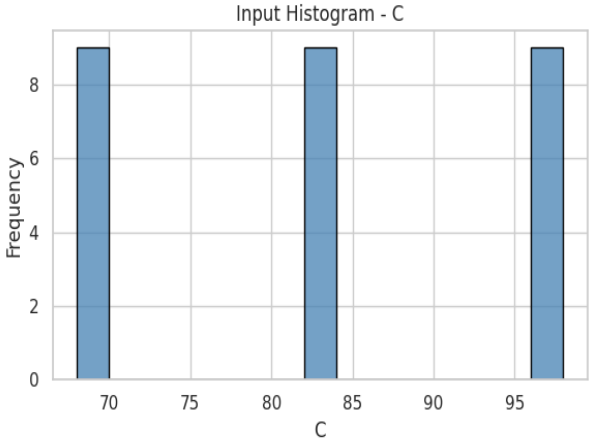

Figure 5.1. (c) Input histogram of particle size of red mud

The output histograms for experimental flexural and impact strength (Figure 5.2) reveal a broad yet continuous distribution, indicating strong sensitivity of mechanical properties to the selected control parameters. Flexural strength varies from approximately 32 MPa to 51 MPa, while impact strength ranges from 28 J/m to 43 J/m, highlighting the competing and non-linear effects of fibre loading, filler content, and particle size.

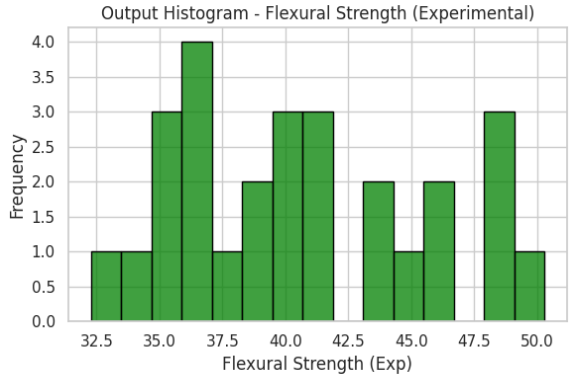

Figure 5.2. (a) Output histogram for Experimental Flexural

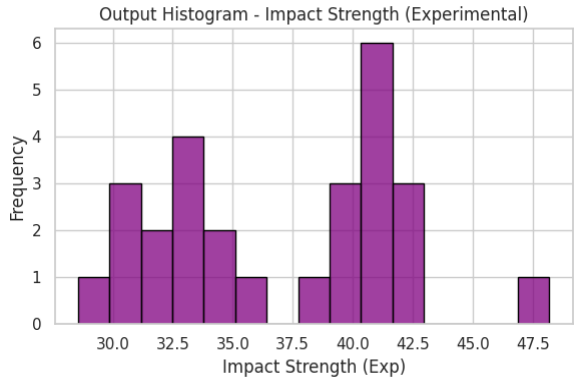

Figure 5.2. (b) Output histogram for Impact Strength.

Genetic Algorithm (GA) Prediction Performance

The GA-predicted output distributions (Figure 5.3) closely resemble the experimental histograms, suggesting that the algorithm successfully captured the underlying non-linear relationships between input parameters and mechanical responses. The box plots (Figure 5.4) further confirm this

observation, showing near-identical medians and interquartile ranges between experimental and predicted datasets observation,

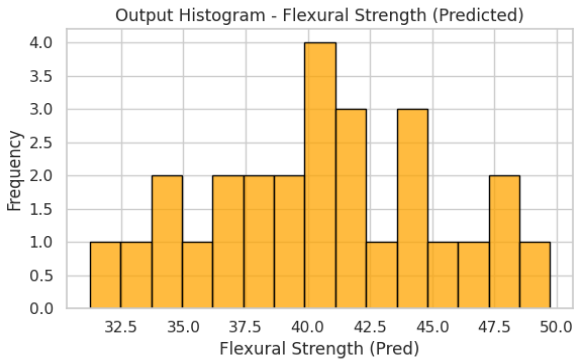

Figure 5.3. (a) Output histogram for Predicted Flexural strength

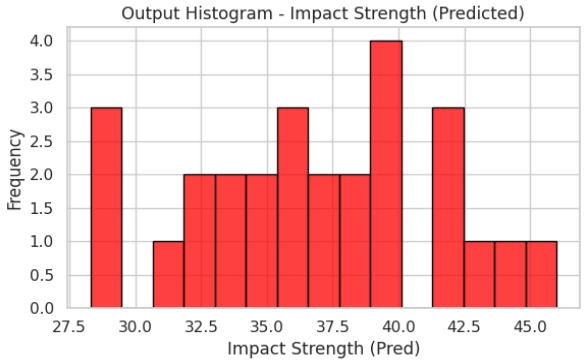

Figure 5.3. (b) Output histogram for Predicted Impact strength

Figure 5.4 (a) compares the experimental and GA-predicted values Using boxplots. The close alignment of medians and interquartile ranges demonstrates minimal deviation between experimental and predicted results. The absence of large outliers reflects the GA model's robustness and its ability to prevent overfitting.

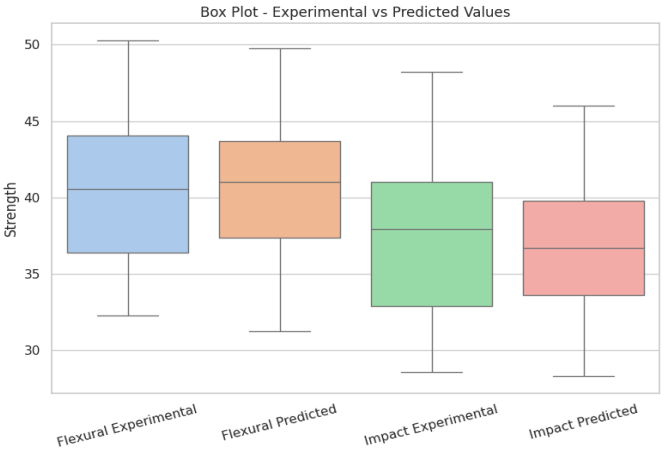

Figure 5.4 (a) Box plot showing variances between the experimental and predicted values

Figures 5.5 (a) and (b) Both plots display strong positive correlations, forming a nearly linear trend. The clustering around the line of equality (y = x) indicates excellent prediction accuracy. Scatter plots for flexural and impact strength (Figures 5.5a–b) exhibit strong linear correlation with minimal dispersion around the unity line, resulting in high coefficients of determination ($R^2 = 0.930$ for flexural strength and 0.886 for impact strength). This superior performance in flexural strength prediction can be attributed to GA's strong global search capability and effective genetic operators, which are particularly well-suited for exploring complex parameter interactions governing bending-dominated behavior in hybrid composites.

Figure 5.5 (a) Scatter plot showing the correlation between

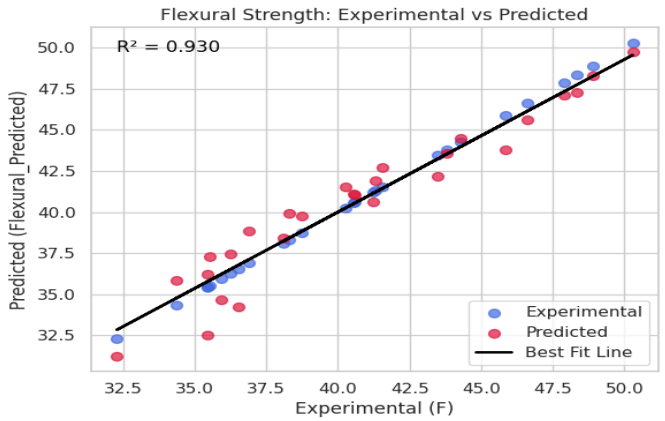

experimental and predicted values for Flexural Strength.

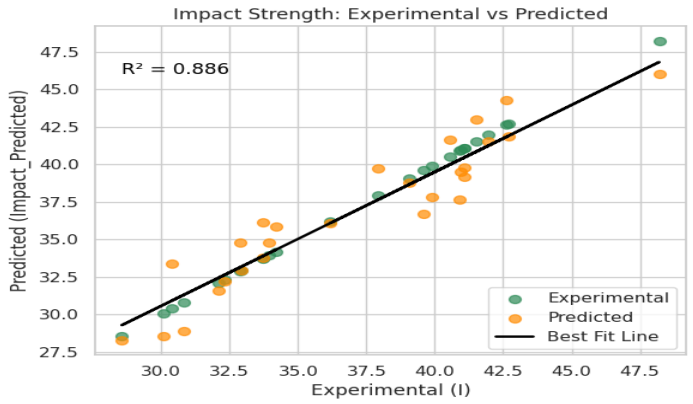

Figure 5.5 (b) Scatter plot showing the correlation between experimental and predicted values for Impact Strength.

Differential Evolution Algorithm(DE) Prediction Performance

Figures 5.6 (a) and (b) illustrate the Differential Evolution (DE) algorithm's predicted results. Although the general shape resembles the experimental distribution, DE shows slightly wider spread and

minor deviation in peak frequencies, indicating higher prediction uncertainty.

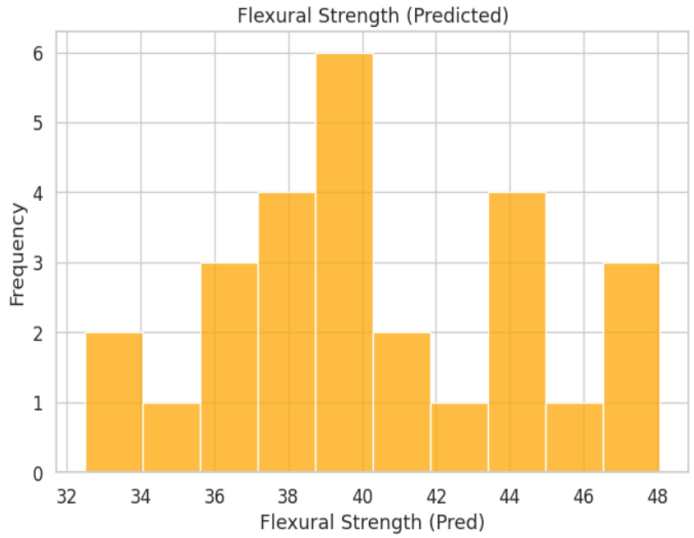

Figure 5.6(a) Output histogram for predicted Flexural Strength by DE

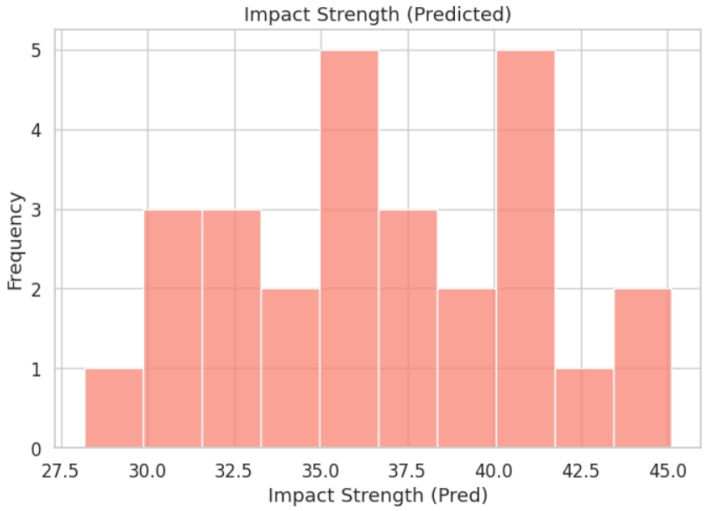

Figure 5.6(b) Output histogram for predicted Impact Strength by DE

The DE box plot (Figure 5.7 a) highlights a noticeable difference between experimental and predicted medians.While the variance remains within acceptable limits, the wider boxes indicate greater error margins compared to GA.

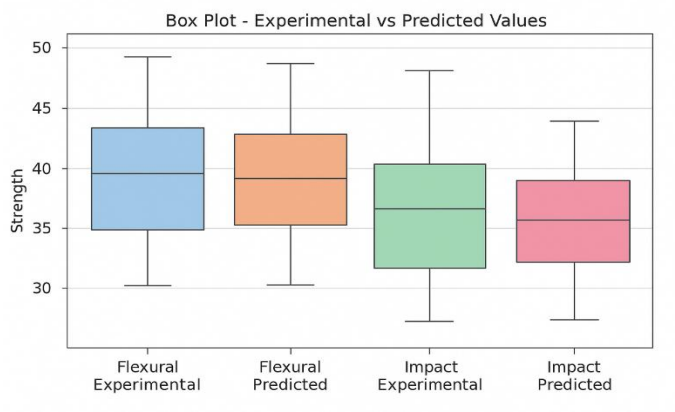

Figure 5.7 (a) Box plot showing variances between the experimental and predicted values for DE.

Figures 5.8 (a) and (b) show that this visual dispersion corresponds to the computed $R^2 = 0.8518$ (flexural) and 0.8405 (impact), confirming a slightly weaker predictive performance.

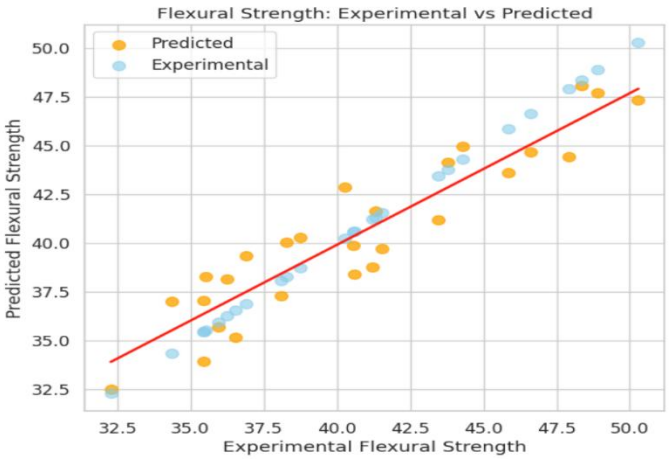

Figure 5.8 (a) Scatter plot showing the correlation between experimental and predicted values for Flexural Strength by DE.

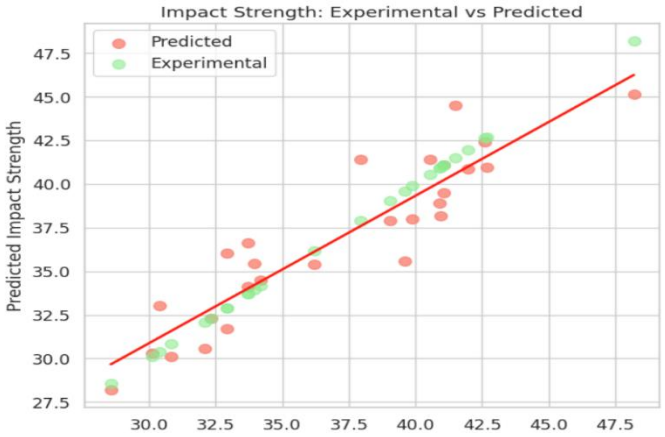

Figure 5.8 (b) Scatter plot showing the correlation between experimental and predicted values for Impact Strength by DE.

Gray Wolf Optimization (GWO) Prediction Performance

Figures 5.9 (a) and (b) show the histogram shapes closely mirror experimental distributions, demonstrating good model accuracy.For impact strength, the GWO curve overlaps almost entirely with the experimental histogram.

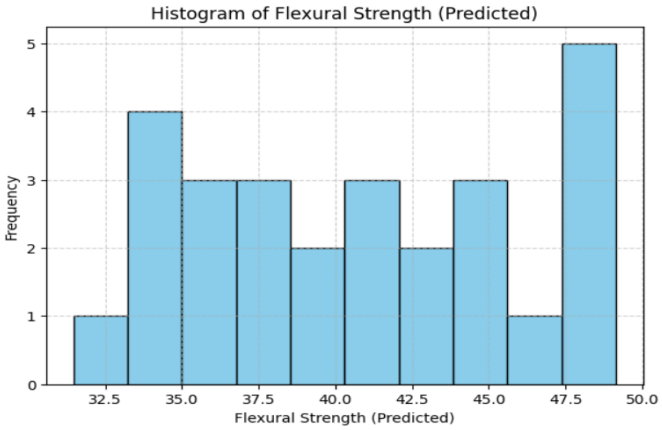

Figure 5.9(a) Output histogram for predicted Flexural Strength by GWO.

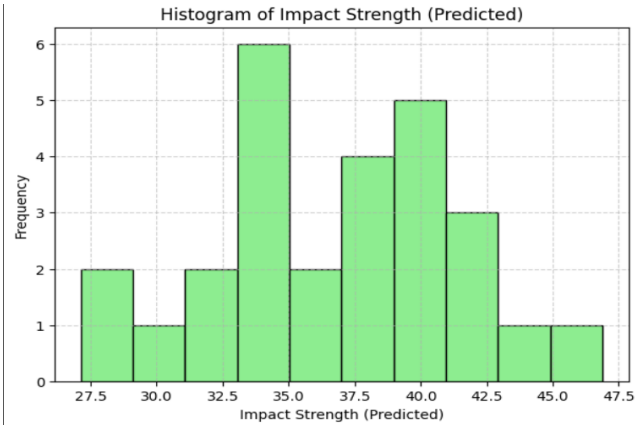

Figure 5.9(b) Output histogram for predicted Impact Strength by GWO.

Figure 5.10(a) presents the variance comparison between experimental and GWO-predicted data. The box heights are small, and medians coincide with experimental values, indicating narrow prediction spread. This uniformity confirms that the GWO model maintained balanced accuracy for both flexural and impact strengths, with minimal statistical deviation.

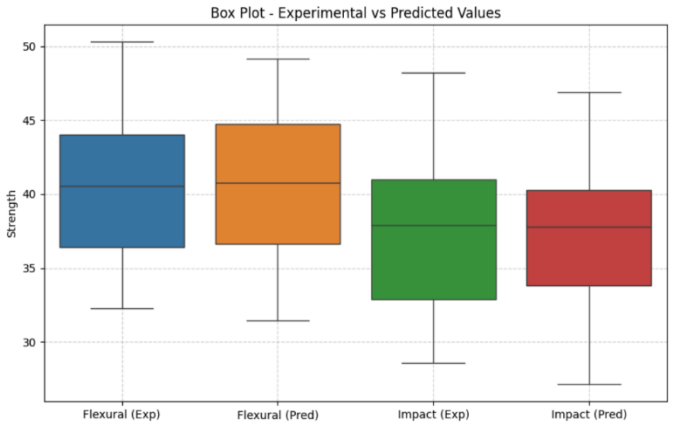

Figure 5.10 (a) Box plot showing variances between the experimental and predicted values for GWO.

Figures 5.11 (a) and (b) illustrate the correlation between experimental and predicted values from the GWO algorithm.The tight clustering of data points along the unity line for *Impact Strength* proves GWO's superior precision for this property.For *Flexural Strength*, the correlation remains high

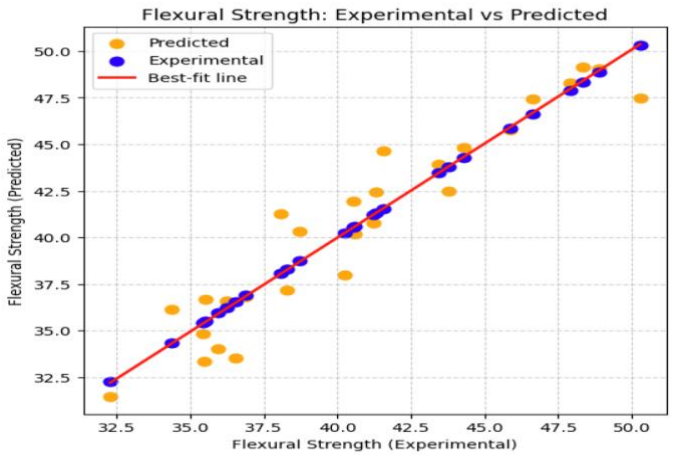

Figure 5.11 (a) Scatter plot showing the correlation between experimental and predicted values for Flexural Strength by GWO.

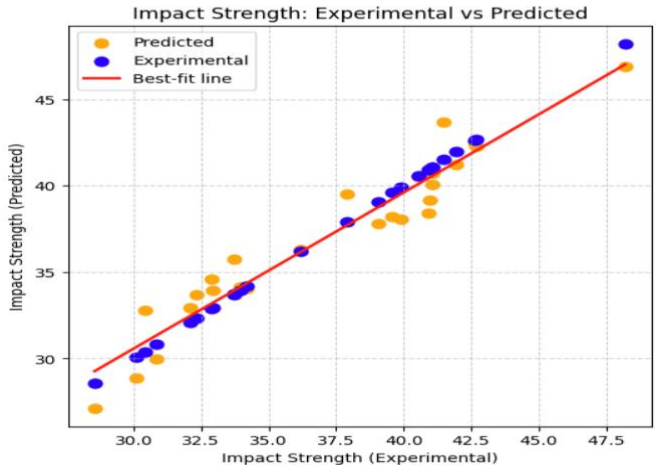

Figure 5.11 (b) Scatter plot showing the correlation between experimental and predicted values for Impact Strength by GWO.

Comparative Algorithmic Performance

Table 5.1 summarizes the predictive performance of all three algorithms. While all methods achieved acceptable accuracy ($R^2 > 0.84$), clear distinctions emerge:

- **GA** demonstrated the highest accuracy for flexural strength prediction ($R^2 = 0.930$).
- **GWO** outperformed other methods in impact strength prediction ($R^2 = 0.9258$).
- **DE**, although effective, consistently exhibited lower predictive accuracy for both properties.

These findings confirm that algorithm performance is property-dependent, and no single heuristic method is universally optimal for all mechanical responses. The results also reinforce the limitations of relying on a single optimization approach when dealing with multi-physics material behaviour.

S.no	Algorithms	R^2 (Flexural Strength)	R^2 (Impact Strength)
1	GA	0.930	0.886
2	DE	0.8518	0.8405
3	GWO	0.8971	0.9258

Table 5.1. Performance Matrix Evaluation

Discussion

A comparative analysis of the three optimization algorithms revealed distinct and specialized predictive capabilities for flexural and impact strength. The Genetic Algorithm (GA) clearly excelled in predicting Flexural Strength, achieving the highest Coefficient of Determination (R^2=0.930) of any model for that property. This strong quantitative result confirms the exceptionally tight clustering of data points observed in its corresponding scatter plot (Page 1). While the GA was also highly effective for Impact Strength (R^2=0.886), its performance in that category was surpassed by the Hybrid Grey Wolf Optimization (GWO) model. The GWO model proved to be the superior predictor for Impact Strength, yielding a top-performing R^2 of 0.9258 and also demonstrated robust accuracy for Flexural Strength (R^2=0.8971). In contrast, the Differential Evolution (DE) model, while still providing good correlations, was consistently the least accurate of the group. It yielded the lowest R^2 values for both flexural (0.8518) and impact (0.8405) strength, a finding supported by the more significant data scatter visible in its plots (Pages 3-4). In summary, while all three models demonstrated efficacy (all $R^2 > 0.84$), the GA and GWO models are clearly superior, offering specialized and more accurate performance depending on the target property.

Conclusion

This study successfully evaluated the predictive performance of three optimization algorithms Genetic Algorithm (GA), Differential Evolution (DE), and a hybrid Grey Wolf Optimization (GWO) model—for estimating the flexural and impact strength of the material.

Based on the quantitative analysis of the results, the following conclusions are drawn:

1. All three models demonstrated good predictive capabilities, achieving Coefficient of Determination (R^2) values greater than 0.84 for both mechanical properties.
2. The Differential Evolution (DE) + ANOVA model was consistently the least accurate of the three, yielding the lowest R^2 values for both flexural strength (0.8518) and impact strength (0.8405).
3. The Genetic Algorithm (GA) was identified as the optimal model for predicting Flexural Strength, achieving the highest R^2 value in the study at 0.930.
4. The Hybrid GWO model proved to be the superior model for predicting Impact Strength, registering a top-performing R^2 of 0.9258.
5. The findings clearly indicate that the choice of the optimal algorithm is property-dependent. For applications where flexural strength is the critical parameter, the GA model is recommended. Conversely, for applications prioritizing impact strength, the Hybrid GWO model is the recommended choice.

References

1. [1] M. Jawaid and H. P. S. A. Khalil, “Cellulosic/synthetic fibre reinforced polymer hybrid composites: A review,” *Polymers*, vol. 13, no. 20, p. 3514, 2021.
2. [2] T. Islam, M. H. Chaion, et al., “Advancements and challenges in natural fiber-reinforced hybrid composites: A comprehensive review,” *SPE Polymers*, 2024.
3. [3] S. Prasad and M. Sain, “Applications of natural fiber composites in automotive and packaging industries: A review,” *Polymers*, vol. 15, no. 3, p. 612, 2023.
4. [4] I. McKay, J. Vargas, L. Yang, and R. M. Felfel, “A review of natural fibres and biopolymer composites: Progress, limitations, and enhancement strategies,” *Materials*, vol. 17, no. 19, p. 4878, 2024.
5. [5] “Mechanical performance and durability attributes of biodegradable natural fibre-reinforced composites—a review,” *J. Materials Science: Materials in Engineering*, 2024.
6. [6] F. Sarker, P. Potluri, et al., “Ultra-high performance of nano-engineered graphene-based natural jute fiber composites,” *arXiv preprint*, arXiv:1905.00750, 2019.
7. [7] A. Rao, T. Divoux, et al., “Printable, castable, nanocrystalline cellulose-epoxy composites exhibiting hierarchical nacre-like toughening,” *arXiv preprint*, arXiv:2108.08747, 2021.
8. [8] Coatings Journal, “Plant-based natural fibre reinforced composites: Fabrication, properties and applications,” *Coatings*, vol. 10, no. 10, p. 973, 2020.

9. [9] M. A. Paglicawan, et al., “Mechanical Properties of Abaca–Glass Fiber Composites,” *Polymers*, 2021.
10. [10] M. Cai, et al., “Effect of Alkali Treatment on Interfacial Bonding in Abaca Fiber-Reinforced Composites,” *Composites Part B: Engineering*, 2016.
11. **[11] A. K. Sinha, et al., “Experimental Determination and Modelling of the Mechanical Properties of Hybrid Abaca-Reinforced Polymer Composite Using RSM,” *Proc. IMechE, Part L: Journal of Materials: Design and Applications*, 2019.**
12. [12] M. A. Altaee, et al., “Mechanical Properties of Interply and Intraply Hybrid Laminates with Abaca/Jute/Glass,” *Journal of Engineering and Applied Science*, 2023.
13. [13] B. V. Ramnath, et al., “Experimental Investigation on Shear and Hardness of Abaca-Raffia Hybrid Composite,” *MATEC Web of Conferences*, 2016.
14. [14] A. P. Irawan, et al., “An Experimental Investigation into Mechanical and Viscoelastic Properties of Hybrid Natural-Fiber Composites,” *Polymers*, 2022.
15. [15] F. Seculi, et al., “The Case of Abaca-Fiber-Reinforced Bio-Polyethylene (BioPE): Flexural Properties,” *Polymers*, 2023.
16. [16] F. Seculi, et al., “Comparative Evaluation of the Stiffness of Abaca-Fiber-Reinforced BioPE and HDPE,” *Polymers*, 2023.
17. [17] S. Alcívar-Bastidas, et al., “Characterization and Life-Cycle Assessment of Alkali-Treated Abaca Fibers with NaOH Recirculation,” *Construction and Building Materials*, 2024.
18. [18] S. Rajendran, G. Palani, N. B. Karthik Babu, A. Veerasimman, Yo-Lun Yang, Vigneshwaran Shanmugam, “Investigation on Erosion Resistance in Polyester–Jute Composites Reinforced with Jute Fibers and Red Mud Particulates,” *Polymers*, 2024.
19. [19] L. Melnyk, “Enhanced Impact Strength of Glyptal Resin Composites with Red Mud: A Comparative Study of Incorporation Methods,” *Technologies and Engineering*, vol. 25, no. 6, pp. 61–68, 2024.
20. [20] A. J. G. dos Santos, M. M. Ribeiro, A. d. C. Corrêa, J. d. S. Rodrigues, D. S. Silva, R. F. P. Junio, S. N. Monteiro, “Investigation of the Flexural and Tensile Properties of Hybrid Polyester Composites Reinforced with Bamboo Fibers and Red Mud Waste,” *Polymers*, vol. 17, no. 8, p. 1060, 2025.
21. [21] Box, G. E. P., & Wilson, K. B. (1951). On the experimental attainment of optimum conditions. *Journal of the Royal Statistical Society: Series B (Methodological)*, 13(1), 1–45.
22. [22] Myers, R. H., Montgomery, D. C., & Anderson-Cook, C. M. (2016). Response Surface Methodology: Process and Product Optimization Using Designed Experiments (4th ed.). Wiley.
23. [23] Iliyasu, M. I., Sapuan, S. M., Ibrahim, K. A., & Azaman, M. D. (2022). Response surface methodology for the optimization of the effect of fibre parameters on the physical and mechanical properties of deleb palm fibre reinforced epoxy composites. *Journal of Materials Research and Technology*, 18, 4567–4579.
24. [24] Dewangan, S., Sharma, S., & Sahu, R. (2025). Multi-objective optimization of hybrid composite laminates using response surface methodology and AHP–TOPSIS approach. *Journal of Composite Materials*, 59(3), 785–798.
25. [25] Ma, L., Zhang, Y., & Xu, H. (2024). Optimization of mechanical and thermal properties of grass-fiber-reinforced composites using response surface methodology. *Materials*, 17(15), 3703.
26. [26] Kaplan, M., Çakır, F., & Kaya, M. (2025). Experimental and statistical optimization of ceramic-filled polyester resin composites using response surface methodology. *Journal of Materials Science: Materials in Electronics*, 36(2), 11456–11470.
27. [27] Ajmal, M., Mohammed, F., & Raghavendra, G. (2024). Cryogenic treatment and nanofiller optimization of flax fiber composites using response surface methodology. *Frontiers in Materials*, 11, 1344351.
28. [28] Montgomery, D. C. (2017). *Design and Analysis of Experiments* (9th ed.). Wiley.
29. [29] Sebaey, T. A., Lopes, C. S., Blanco, N., & Costa, J. (2011). Ant colony optimization for dispersed laminated composite panels under biaxial loading. *Composite Structures, 93*(8), 2135–2144. https://doi.org/10.1016/j.compstruct.2011.03.018
30. [30] Hwang, S. F. (2014). A genetic algorithm for the optimization of fiber angles in composite laminates. *International Journal of Precision Engineering and Manufacturing*, 15(6), 1163–1171. https://doi.org/10.1007/s12206-014-0725-y
31. [31] Le-Manh, T., & coauthors. (2014). Stacking sequence optimization of laminated composite structures using GA and isogeometric analysis. *Composite Structures*. https://doi.org/10.1016/j.compstruct.2014.05.011
32. [32] Ho-Huu, V., & Nguyen, T. (2016). Optimization of laminated composite plates for maximizing buckling load using improved differential evolution and smoothed FEM. *Composite Structures, 153*, 574–585. https://doi.org/10.1016/j.compstruct.2016.06.005
33. [33] Cakiroglu, C., & coauthors. (2020). Harmony search optimisation of dispersed laminated composite plates for buckling load maximisation. *Materials, 13*(14), 3069. https://doi.org/10.3390/ma13143069
34. [34] Arjomandi, M. A., Shishehsaz, M., Ghanbarzadeh, A., Mosallanezhad, B., & Akrami, M. (2022). Application of Particle Swarm Optimization for improvement of peel strength in a laminated double-lap composite joint. *Applied Sciences, 12*(14), 6997. https://doi.org/10.3390/app12146997
35. [35] Wang, Z. Z., & Wu, X. (2020). A comparative review of genetic algorithms in optimisation of composite materials and structures. *Composite Structures*. https://doi.org/10.1016/j.compstruct.2019.111234
36. [36] Emambocus, B. A. S., Mirjalili, S., & others. (2021). Dragonfly algorithm and its hybrids: a survey on performance, objectives and applications. *Sensors, 21*(22), 7542. https://doi.org/10.3390/s21227542
37. [37] Parmaksiz, H., Yuzgec, U., Dokur, E., & Erdogan, N. (2023). Mutation-based improved dragonfly optimization algorithm for a neuro-fuzzy system in short term wind speed forecasting. *Knowledge-Based Systems, 268*, 110472. https://doi.org/10.1016/j.knosys.2023.110472
38. [38] Wang, L., Shi, Y., & Zhang, X. (2021). Angle-modulated Dragonfly Algorithm for binary combinatorial optimization. *Entropy, 23*(5), 598. https://doi.org/10.3390/e23050598
39. [39] Liu, X., Wang, Z., & Zhang, Y. (2023). Parallel layup optimization method for matching lamination parameters. *Composite Structures, 302*, 116475. https://doi.org/10.1016/j.compstruct.2022.116475
40. [40] Zadeh, P. M., & coauthors. (2018). Bi-level optimization of laminated composite structures for manufacturable lightweight design. *Journal of Mechanical Science and Technology*. https://doi.org/10.1007/s12206-018-0319-1
41. [41] Optimization of buckling load for laminated composite plates using adaptive Kriging-improved PSO: A novel hybrid intelligent method

42. [42] Malashin, I., & coauthors. (2024). Multi-objective evolutionary tuning of neural network surrogates for textile-composite property prediction. *Polymers*. https://doi.org/10.3390/polym14081700
43. [43] Yibre, A. M., & Tekalign, H. (2020). Weight optimization of hybrid composite laminates using an artificial algae algorithm. *SN Applied Sciences, 2*, 3126. https://doi.org/10.1007/s42452-020-3126-0
44. [44] Işık, M. F., & coauthors. (2023). Hybrid ANN–PSO approach for composite structural prediction and layup optimization. *Sustainability, 15*(12), 9715. https://doi.org/10.3390/su15129715
45. [45] Qu, S., Liu, F., & Cao, Z. (2024). An adaptive surrogate-assisted particle swarm optimization algorithm combining global and local surrogate models. *Applied Sciences, 14*(17), 7853. https://doi.org/10.3390/app14177853
46. [46] ue, J., & coauthors. (2024). A damage imaging method for composites based on particle swarm optimization and guided ultrasonic waves. *Composite Structures*. https://doi.org/10.1016/j.compstruct.2024.120XXX (DOI to confirm). ScienceDirect
47. [47] Li, F., & coauthors. (2020). A fast surrogate-assisted particle swarm optimization (FSAPSO) for computationally expensive design problems. *Engineering Applications of Artificial Intelligence* (DOI to confirm). ScienceDirect